Recent Progress of Neutron Spectrometer Development for LHD Deuterium Plasmas*)

Mitsutaka ISOBE[1,2], Kunihiro OGAWA[1,2], Siriyaporn SANGAROON[3], Guoqiang ZHONG[4] and Tieshuan FAN[5]

[1]*National Institute for Fusion Science, National Institutes of Natural Sciences, Toki 509-5292, Japan*
[2]*The Graduate University for Advanced Studies, SOKENDAI, Toki 509-5292, Japan*
[3]*Faculty of Science, Mahasarakham University, Maha Sarakham 44150, Thailand*
[4]*Institute of Plasma Physics, Chinese Academy of Sciences, Hefei 230031, People's Republic of China*
[5]*State Key Laboratory of Nuclear Physics and Technology, Peking University, Beijing 100871, People's Republic of China*

(Received 10 January 2022 / Accepted 31 January 2022)

The commissioning of three different types of D-D neutron energy spectrometer has been performed in the Large Helical Device (LHD) to accelerate energetic-ion physics studies in a non-axisymmetric system. Because the LHD is equipped with negative-ion-source-based tangential neutral beam injectors (N-NBs) characterized by high energy up to 180~190 keV, a significant Doppler shift of D-D neutron energy from 2.45 MeV is expected. Two different compact neutron energy spectrometers, i.e., a conventional liquid organic scintillator, designated as EJ-301, and a newly developed Cs_2LiYCl_6:Ce with ^{7}Li-enrichment called CLYC7, having tangential sightlines, have shown up- and/or down-shifted D-D neutron energy, as expected according to the direction of N-NB injection. In addition, with the aim of study on a perpendicular energetic ion tail, created by wave heating with ion cyclotron resonance frequency, a neutron energy spectrometer named the Time of Flight Enhanced Diagnostic (TOFED) is being developed. The TOFED is based on a time-of-flight technique and is characterized by high-energy-resolution and a high-counting-rate capability. Commissioning of the TOFED is now ongoing. Recent advances of neutron energy spectrometer development for LHD deuterium plasmas are described.

Keywords: LHD, NBI, deuterium plasma, energetic ion, neutron, Doppler shift

DOI: 10.1585/pfr.17.2402008

1. Introduction

D-D and D-T born fusion neutron energies are often referred to as 2.45 MeV and 14.1 MeV, respectively, originating in those Q-values. However, the actual birth neutron energy in a fusion plasma is not monoenergetic, since the neutron energy reflects the relative velocity of two colliding fuel ions. At the dawn of fusion research, neutron spectrometry was proposed as the tool of a fuel ion temperature diagnostic through the measurement of Doppler broadening of neutron energy [1–3]. However, in a high-temperature plasma heated auxiliary by neutral beam (NB) injection and/or an ion cyclotron range of frequency (ICRF) wave, fuel ions' velocity distribution is no longer Maxwellian. As a result, the neutron energy spectrum is strongly affected by the velocity distribution function of energetic fuel ions. In other words, neutron spectrometry can work as a tool of energetic-ion diagnostics for a fusion plasma [4, 5]. Also, it is shown that neutron spectrometry can be used potentially as a tool of plasma rotation measurement [6]. Facing an age of burning plasmas such as the ITER [7] and the Chinese Fusion Engineering Testing Reactor called CFETR [8], the role of neutron spectrometry is becoming increasingly important.

The velocity distribution function of confined energetic ions is of inherent interest for deeper understanding of physics related to energetic ions such as the slowing-down process and energetic-ion-driven magnetohydrodynamics (MHD) instabilities. For this reason, various types of neutron energy spectrometers (NESs) for D-D and D-T neutrons have been developed and operated in tokamaks [9–16]. As the start of the deuterium discharge in the Large Helical Device (LHD) [17], the LHD has been operated with a comprehensive set of neutron diagnostics [18–21]. However, only an NES has been lacking. In order to enhance energetic-ion physics research in the LHD, we have been developing three different neutron spectrometers, i.e. two different compact neutron energy spectrometers (CNESs) based on a conventional liquid organic scintillator called EJ-301 [22] and a newly developed Cs_2LiYCl_6:Ce with ^{7}Li-enrichment (CLYC7) [23, 24], and a large-sized neutron spectrometer named the Time of Flight Enhanced Diagnostic (TOFED) based on a time-of-flight technique with high-energy-resolution and a high-counting-rate capability [25, 26]. In this paper, recent

author's e-mail: isobe.mitsutaka@nifs.ac.jp

*) This article is based on the presentation at the 30th International Toki Conference on Plasma and Fusion Research (ITC30).

progress of D-D neutron spectrometer development in the LHD and representative results are described.

2. Experimental Setup

Two CNESs, i.e. the EJ-301 and CLYC7 fast-neutron scintillation detectors embedded in a thick radiation shield made of 10% borated polyethylene and lead were installed in the vicinity of the LHD to have a tangential line of sight. Arrangement of the two CNESs is schematically depicted in Fig. 1.

The two scintillation detectors were vertically aligned at the same location. Information on the local detectors' arrangement and radiation shield is available in Ref. [24]. The LHD is equipped with three negative-ion-source-based tangential NB injectors (N-NBIs), characterized by high energy up to 180~190 keV [27]. The two N-NBIs, oriented in opposite directions, were utilized in this study to check the performance of the CNESs. In this case, energy of D-D neutrons resulting from the so-called beam-plasma reaction is expected to be up- and down-shifted from 2.45 MeV at the CNESs, according to the direction of N-NB injection, i.e. circulating energetic deuterons in a deuterium plasma of the LHD. The EJ-301 is a liquid organic scintillator containing plenty of hydrogen atoms and detects fast neutrons through measurement of energetic protons recoiled inside the scintillator. Note that even if the incident fast neutron is monoenergetic, the recoil proton's energy is widely distributed according to angles of elastic scattering [28]. Therefore the response function of the detector to a specific energy of neutrons has to be known, and an unfolding technique is required to reconstruct the energy of incident neutrons. Prior to measurement in the LHD, we obtained the detector's response function for the EJ-301 detector at the Fast Neutron Laboratory (FNL) of Tohoku University [29]. Unlike the EJ-301, ^{35}Cl(n, p)^{35}S and ^{35}Cl(n, α)^{32}P nuclear reactions are utilized in the case of the CLYC7 and a neutron spectrum can be obtained directly from the energy measurement of reaction products. Fundamental properties of the EJ-301 and CLYC7 are summarized in Table 1. Each fast-neutron scintillator is connected to a photomultiplier tube, hereafter PMT, (H10580-100-01, Hamamatsu Photonics K.K.), embedded in 10 mm thick iron to protect from any stray magnetic field, and an anode signal is directly fed into a sophisticated digitizer, having the capability of pulse shape discrimination (PSD) between neutrons and γ-rays (APV8102-14MWPSAGb, Techno AP (14 bits, 1 GHz sampling) for the EJ-301, and DT5720B, CAEN (12 bits, 250 MHz sampling) for the CLYC7).

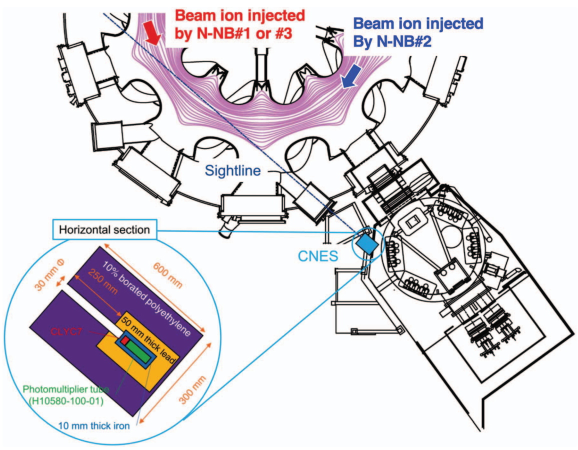

Fig. 1 Arrangement of two compact neutron energy spectrometers. Size and materials of radiation shield, and collimator size are given. Direction of N-NB injection in this experiment is also depicted.

Unlike CNESs, aiming at measurement of neutron energy broadening due to perpendicular energetic ions kicked by the ICRF wave heating, the TOFED is installed in the basement of the LHD torus hall, having a vertical line of sight through a heavy concrete collimator, embedded into the concrete floor of the torus hall [26].

3. Experimental Results from CNESs

Both CNESs have successfully shown the dynamics of circulating beam deuterons, i.e. Doppler-shifted neutron energy associated with the direction of circulating beam deuterons has been clearly observed as expected. Waveforms of a discharge for measurement of the neutron energy spectrum by the EJ-301 are shown in Fig. 2. In this particular shot, neutral beams are perpendicularly injected by P-NB#4 and #5, tangentially counter-injected by N-NB#2, and co-injected by N-NB#3 separately into the background deuterium plasma, sustained by electron cyclotron resonance heating (ECRH). Here, the P-NB means a positive-ion-source-based NB. Note that the EJ-301 scintillation detector can be operated properly without suffering pulse pile-up up to a total neutron emission rate (S_n) of 6×10^{13} (n/s).

Recoil proton energy spectra inside the EJ-301 scintillator and D-D neutron energy distribution for three different NB injection patterns are shown in Figs. 3a) and 3b),

Table 1 Fundamental properties of fast-neutron scintillators employed in the LHD.

	EJ-301	CLYC7
Material	xylene-and naphthalene-based organic liquid	Cs_2LiYCl_6:Ce with enriched ^{7}Li
Reaction	Elastics neutron-proton scattering	^{35}Cl(n,p)^{35}S, ^{35}Cl(n,a)^{32}P
Decay time	< 10 ns	~ 1 μs
Peak wavelength	425 nm	370 nm
Scintillator size	ϕ=1 inch, l=1 inch	ϕ=1 inch, l=1 inch

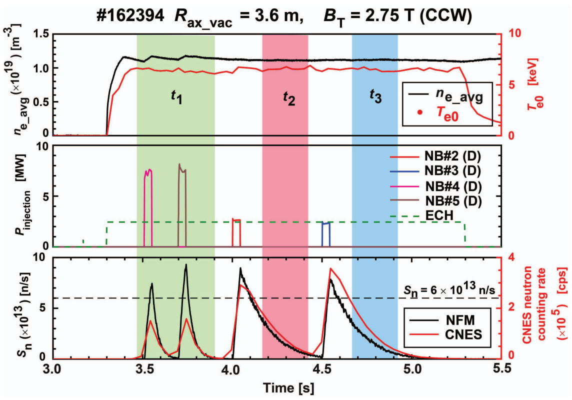

Fig. 2 Waveforms of line-averaged electron density, neutral beam injection, electron cyclotron resonance heating, neutron emission rate measured with neutron flux monitor (NFM) based on ^{235}U fission chamber, and neutron counting rate measured with EJ-301 scintillation detector.

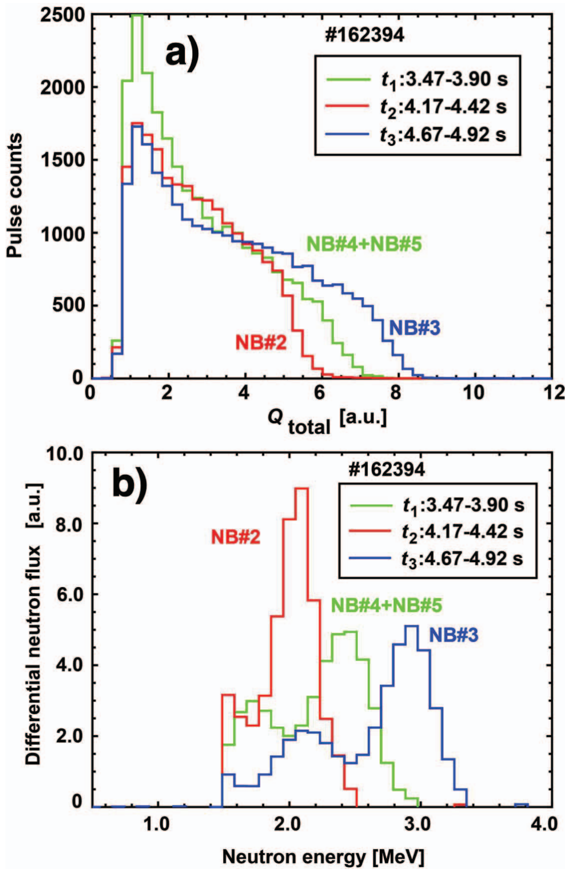

Fig. 3 a) Recoil proton energy spectra inside EJ-301 fast neutron scintillator. Here, the total charge of a pulse signal Q_{total} is proportional to recoil proton energy. b) D-D neutron energy distribution evaluated from recoil proton energy spectra shown in Fig. 3 a) for co-, counter-, and perpendicular injection cases.

respectively. In this analysis, a simple method of the unfolding neutron energy spectrum, described in Ref. [30] and response function coefficients given in Ref. [31], are

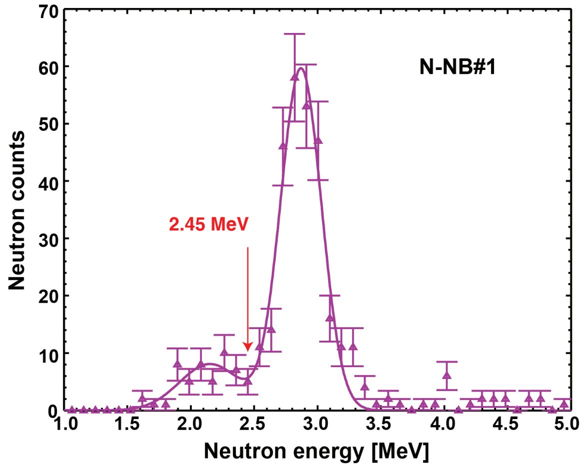

Fig. 4 Doppler-shifted D-D neutron energy measured with CLYC7 detector. Up-shift of D-D neutron energy is clearly observed when N-NB#1 is tangentially injected in counterclockwise direction.

adopted. In the case of tangential N-NB#3 injection, D-D neutron energy was up-shifted from 2.45 MeV as expected, since beam deuterons move toward the EJ-301 detector. On the other hand, down-shifted D-D neutron energy was observed when tangential N-NB#2 was injected because beam deuterons move away from the EJ-301. It can also be seen that the peak energy of D-D neutrons was close to 2.45 MeV when P-NB#4 and #5 were perpendicularly injected. The Doppler-shifted peak energy of D-D neutrons is consistent with that evaluated from the two-body kinematic calculation. The calculation, considering a slowing-down distribution of beam deuterons, is ongoing.

Next, the Doppler-shifted D-D neutron energy measured with the CLYC7 detector is shown in Fig. 4. N-NB#1 is tangentially co-injected in this discharge. In this case, beam deuterons are circulating in a counterclockwise direction, in other words, the direction of beam ion movement faces the CLYC7. An up-shift of D-D neutron energy is clearly observed, as expected. The peak energy of 2.87 MeV matches the energy evaluated by the two-body kinematic calculation.

4. Current Status of TOFED

In contrast to CNESs, the TOFED provides the incident neutron energy by the time difference between the first and second detectors. The TOFED consists of many fast-neutron plastic scintillation detectors, in order to enhance its detection efficiency. The detection principle is available in Ref. [26]. Here, we show the entire view of the TOFED developed for the LHD in Fig. 5.

Five EJ-228 fast-timing plastic scintillators [32] with a diameter of 40 mm, and 6 mm thick, stacked vertically, are employed in the first detector. Each scintillator is equipped with two light guides leading the scintillation light to the two PMTs (H10580, Hamamatsu Photonics K.K.). A set

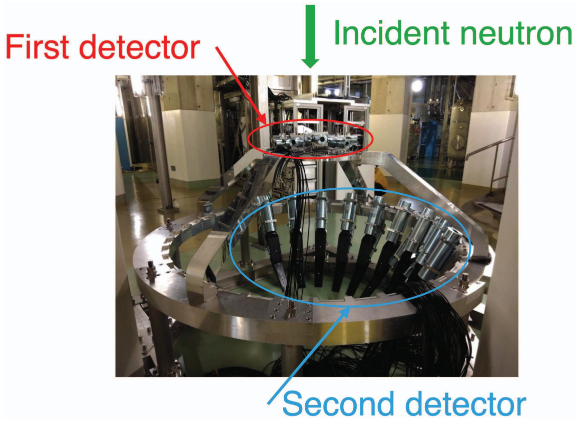

Fig. 5 Entire view of TOFED installed in basement of the LHD torus hall.

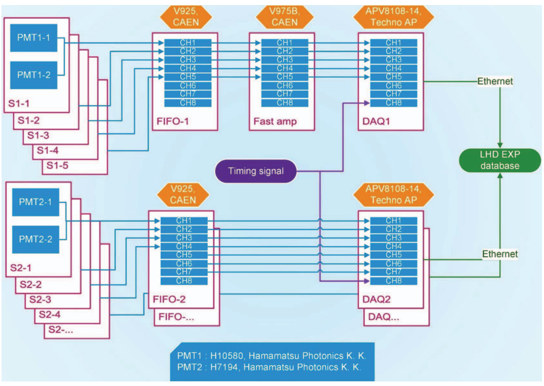

Fig. 6 Electronics employed for TOFED on LHD.

of anode signals from the two PMTs is combined with a fast-in-fast-out module (V925, CAEN) and amplified ten times with a fast amplifier module (V975B, CAEN) and then fed into an 8-channel 1 GHz sampling sophisticated digitizer (APV8108-14, Techno AP) having the capability of a high-counting-rate operation up to 2×10^6 counts per second for each channel. Forty EJ-200 scintillators ~280 mm in length, 70 mm wide, and 17 mm thick as well as forty EJ-200 scintillators ~235 mm in length, 95 mm wide, and 17 mm thick are employed in the second detector. The reason for employing two-types of second detector is to enhance the detection efficiency compared with original time-of-flight spectrometer called the TOFOR in the JET [15]. Each scintillator is coupled with a PMT (H7195, Hamamatsu Photonics K.K.). A set of anode signals from the two PMTs is combined with a fast-in-fast-out module (V925, CAEN) and then fed into the sophisticated digitizer. The start time of all the digitizers is aligned with an accuracy of less than 1 ns, using a timing signal provided by the LHD central control system. The TOFED can provide not only D-D but also D-T neutron energy spectra with high-energy-resolution, owing to the relatively wide-dynamic range and high-time-resolution capabilities of the digitizer. Electronics adopted into the TOFED are schematically depicted in Fig. 6. Neutron and γ-ray transport calculations in support of the design of the radiation shielding for the TOFED have been completed [33]. The total number of detectors has been enhanced, little by little and year by year, toward the completion of the system, and commissioning of the system is ongoing.

5. Summary

For a deeper understanding of energetic-particle confinement physics, e.g. the slowing-down process of energetic ions and the excitation of energetic-ion-driven MHD instabilities, the installation of NESs has been progressed in the LHD. CNESs having tangential sightlines show the up-and down-shift of D-D neutron energy resulting from the tangential deuterium N-NB injections. The consistency between the Doppler-shift of the energy peak and the two-body kinematic calculation shows the performance of the scintillation-based neutron energy spectrometer. The comparison of the neutron spectrum with that calculated by the orbit following models will reveal the velocity distribution of beam ions confined in the plasma core and exciting Alfvénic instabilities. To understand the confinement of energetic ions trapped in the magnetic valley formed by the twisted helical coils, development and commissioning of the perpendicular TOFED have been gradually advanced yearly. The TOFED will become one of the more powerful tools for understanding the ICRF tail ion confinement in three-dimensional magnetic field devices.

Acknowledgments

This work was supported by the NINS program of Promoting Research by Networking among Institutions (Grant No. 01411702), by Japan-China Cooperation in Fusion Research and Development. We are pleased to acknowledge the assistance of the LHD experiment group and the FNL group of Tohoku University.

Data availability statement

The LHD data can be accessed from the LHD data repository at

https://www-lhd.nifs.ac.jp/pub/Repository_en.html

[1] W.R. Faust and E.G. Harris. Nucl. Fusion **1**, 62 (1960).
[2] G. Lehner and F. Pohl, Z. Phys. **207**, 83 (1967).
[3] H. Brysk, Plasma Phys. **15**, 611 (1973).
[4] T. Elevent, Nucl. Instrum. Methods **185**, 313 (1981).
[5] J. Scheffel, Nucl. Instrum. Methods **224**, 519 (1984).
[6] G. Gorini *et al.*, Rev. Sci. Instrum. **68**, 561 (1997).
[7] B. Bigot, Nucl. Fusion **59**, 112001 (2019).
[8] G. Zhuang *et al.*, Nucl. Fusion **59**, 112010 (2019).
[9] J.D. Strachan *et al.*, Nature **279**, 626 (1979).
[10] T. Elevent and M. Olsson, Nucl. Instrum. Methods Phys. Res. A **238**, 147 (1985).
[11] G. Grosshög *et al.*, Nucl. Instrum. Methods Phys. Res. A **249**, 468 (1986).
[12] J. Källne and H. Enge, Nucl. Instrum. Methods Phys. Res.

A **311**, 595 (1992).
[13] M. Osakabe *et al.*, Rev. Sci. Instrum. **65**, 1636 (1994).
[14] A.V. Krasilnikov *et al.*, Nucl. Instrum. Methods Phys. Res. A **476**, 500 (2002).
[15] M. Gatu Johnson *et al.*, Rev. Sci. Instrum. **77**, 10E702 (2006).
[16] Y. Zhang *et al.*, J. Fusion Energy **40**, 14 (2021).
[17] Y. Takeiri, IEEE Trans. Plasma Sci. **46**, 2348 (2018).
[18] M. Isobe *et al.*, IEEE Trans. Plasma Sci. **46**, 2050 (2018).
[19] M. Isobe *et al.*, Nucl. Fusion **58**, 082004 (2018).
[20] K. Ogawa *et al.*, Nucl. Fusion **59**, 076017 (2019).
[21] K. Ogawa *et al.*, Plasma Fusion Res. **16**, 1102023 (2021).
[22] https://eljentechnology.com/products/liquid-scintillators/ej-301-ej-309
[23] D. Rigamonti *et al.*, JINST **14**, C09025 (2019).
[24] S. Sangaroon *et al.*, JINST **16**, C12025 (2021).
[25] Y.M. Zhang *et al.*, J. Fusion Energy **40**, 14 (2021).
[26] Y.M. Zhang *et al.*, Rev. Sci. Instrum. **92**, 053547 (2021).
[27] Y. Takeiri *et al.*, Fusion Sci. Technol. **58**, 482 (2010).
[28] W.J. Price, *Nuclear Radiation Detection* (McGraw-Hill Book Company, Inc., New York, 1958) p. 273.
[29] M. Baba *et al.*, Nucl. Instrum. Methods Phys. A **376**, 115 (1996).
[30] D. Slaughter and R. Strout, II, Nucl. Instrum. Methods **198**, 349 (1982).
[31] V.V. Verbinski *et al.*, Nucl. Instrum. Methods **65**, 8 (1968).
[32] https://eljentechnology.com/products/plastic-scintillators/ej-228-ej-230
[33] S. Sangaroon *et al.*, Fusion Eng. Des. **166**, 112296 (2021).